Maximum Likelihood Synchronization for DVB-T2 in Unknown Fading Channels

Xin Zhang, Jun Liu, *Member, IEEE*, Hongbin Li, *Senior Member, IEEE*, and Braham Himed, *Fellow, IEEE*

***Abstract*—In this paper, we consider the timing and carrier frequency offset (CFO) estimation problem for digital video broadcasting-second generation terrestrial (DVB-T2) transmissions by utilizing the P1 symbol. Unlike previous studies, an unknown fading channel scenario is considered. Two maximum likelihood (ML) methods are derived by modeling the transmitted signal as a stochastic and, respectively, a deterministic unknown waveform. The proposed stochastic ML (SML) algorithm can jointly estimate the received signal power, time delay, and CFO. By ignoring the presence of null carriers in the P1 symbol, the SML method can be simplified with a lower complexity. Meanwhile, the proposed deterministic ML method is more flexible and computationally simpler compared with the SML method. Numerical results are presented to illustrate the performances of the proposed estimators along with several existing solutions for DVB-T2 signal synchronization. In addition, Cramér–Rao lower bounds are evaluated for the considered estimation problem.**

***Index Terms*—Digital TV broadcast, maximum likelihood estimation, synchronization.**

I. Introduction

TO MEET the growing demand of the high definition television (HDTV), ultra high definition television (UHDTV), and mobile TV services, the digital video broadcasting-second generation terrestrial (DVB-T2) standard [1], an extension of its predecessor digital video broadcasting-terrestrial (DVB-T) standard [2], has been devised and considered for deployment in many areas. The DVB-T2 system transmits compressed digital audio, video, and data through "physical layer pipes" by using orthogonal frequency division multiplexing (OFDM) modulation [3] with concatenated channel coding and interleaving. DVB-T2 offers a higher bit rate than DVB-T, and digital terrestrial television (DTT) systems based on DVB-T2 provide more robustness, flexibility and at least 50 percent more efficiency than any other DTT systems. Due to these advantages, the research on DVB-T2 systems has received significant interest in recent years (see [4]–[18] and references therein).

In digital TV broadcasting systems, the synchronization is of particular importance because its performance significantly affects the zap time during switching channels [13] and consequently the user experience, especially when it comes to the mobile services [11], [15]. Therefore, to rapidly acquire the timing and accurately estimate the carrier frequency offset (CFO), DVB-T2 includes many unique features, one of which is that a preamble denoted *P1 symbol* is adopted at the very beginning of each physical-layer frame [19]. A P1 symbol consists of three sections: the central section is generated by an inverse Fourier transform of a sequence of OFDM symbols, and the other two sections, respectively added before and after the central one, are frequency-shifted repetitions of some samples of the central section. This structure is designed to improve robustness against both false detection and loss of detection caused by long-delayed echoes of the channel or spurious signals, such as continuous-wave interferers [19]. In addition to synchronization, the P1 symbol can be used to identify the DVB-T2 frames and convey the 7-bit information for the transmission mode [7]. In [9] and [12], the P1 symbol is also utilized to do the channel estimation after its capture and decoding.

The time delay and CFO estimation by using the P1 symbol has been previously studied in the literature. Two slightly different cross-correlation (CC) based methods are proposed in [5] and [6] to implement the fast synchronization with low complexity. They provide very similar P1 detection and synchronization performance. In [16]–[18], the performance of the correlation-based method is analyzed in some specific channel conditions, such as the two-tap channels with special delays, mobile satellite channels, and mobile terrestrial channels. On the other hand, despite the fact that the generation of the P1 symbol is similar to an OFDM block whose synchronization has been widely studied [20]–[26], none of these algorithms can be directly applied to the P1 symbol, since the structure of the P1 symbol is different from those of conventional OFDM blocks. In other words, a P1 symbol has two special guard intervals placed before and after the main body, respectively, while a conventional OFDM block only has a cyclic prefix. Extending OFDM-based synchronization studies in [26]–[29], a maximum likelihood (ML) synchronization scheme is proposed in [13] for DVB-T2 by exploiting

Manuscript received June 2, 2014; revised August 28, 2015; accepted September 9, 2015. Date of publication October 16, 2015; date of current version December 5, 2015.

X. Zhang and H. Li are with the Department of Electrical and Computer Engineering, Stevens Institute of Technology, Hoboken, NJ 07030 USA (e-mail: xzhang23@stevens.edu; hongbin.li@stevens.edu).

J. Liu was with the Department of Electrical and Computer Engineering, Stevens Institute of Technology, Hoboken, NJ 07030 USA. He is now with the National Laboratory of Radar Signal Processing, Xidian University, Xi'an 710071, China (e-mail: jun_liu_math@hotmail.com).

B. Himed is with AFRL/RYMD, Dayton, OH 45433 USA (e-mail: braham.himed@us.af.mil).

Color versions of one or more of the figures in this paper are available online at http://ieeexplore.ieee.org.

Digital Object Identifier 10.1109/TBC.2015.2482018

the structure of the P1 symbol. Two simplified algorithms are presented. Simulations show that the proposed methods outperform the correlation-based method. Nevertheless, the problem in [13] is solved under the assumption that the received signal power is known a-priori.

In this paper, we consider the time delay and CFO estimation, by exploiting the special structure of the P1 symbol, over an unknown fading channel. Our study is motivated by the fact that fading is ubiquitous in broadcasting systems due to multipath propagation and shadowing effects from obstacles [30], and the fact that the channel gain is generally unknown to the receiver during the synchronization phase. Two ML synchronization approaches are proposed based on two different models for the transmitted signal. First, based on a stochastic model, we develop a stochastic ML (SML) method which can jointly estimate the received signal power, time delay, and CFO. By further assuming that all sub-carriers in the P1 symbol are active, the SML method is simplified with a lower computational complexity. Second, a deterministic ML (DML) method is proposed by modeling the transmitted signal as unknown deterministic quantities. In contrast with the SML method, the DML method is more flexible in that its implementation is independent of the presence/absence of the null carriers in the P1 symbol. Furthermore, the DML estimator is computationally simpler than the SML estimator, however at a price of reduced estimation accuracy. Numerical results are presented to demonstrate the effectiveness of the proposed methods relative to several existing solutions. Cramér-Rao lower bounds (CRLB) are also assessed for the considered estimation problem in the numerical simulations.

The remainder of the paper is organized as follows. In Section II, we illustrate the particular structure of the P1 symbol and formulate our problem. The ML synchronization algorithms based on the stochastic model and the CRLBs thereof are derived in Section III, and Section IV addresses the deterministic model as well as the corresponding CRLBs. Numerical results and discussions are included in Section V, followed by the conclusion in Section VI.

Notation: Vectors (matrices) are denoted by boldface lower (upper) case letters, and all vectors are column vectors. Superscripts $(\cdot)^*$, $(\cdot)^T$, and $(\cdot)^H$ denote complex conjugate, transpose, and complex conjugate transpose, respectively. $\Re\{\cdot\}$ and $\Im\{\cdot\}$ represent the real and the imaginary parts of a complex quantity, respectively. $E\{\cdot\}$ denotes statistical expectation, j stands for the imaginary unit, $\mathbf{0}_{p\times q}$ denotes a $p\times q$ matrix with all zero entries, $\mathbf{I}_n$ denotes an identity matrix of size n, $\odot$ denotes the Hadamard product, $[\,\cdot\,]_{m,n}$ denotes an entry at the m-th row and the n-th column of a matrix, $\sim$ means "is distributed as," $\mathcal{CN}$ denotes a circularly symmetric, complex Gaussian distribution, $|\cdot|$ represents the determinant (modulus) of a matrix (complex number), and $\mathrm{tr}\{\cdot\}$ denotes the trace of a matrix.

II. Problem Formulation

In DVB-T2 systems, the data transmission is based on frames. At the top level it is organized in T2 superframes, each consisting of a particular number of consecutive T2-frames and probably several future extension frames (FEF). Each T2-frame, as well as the FEF part, always starts with a P1 symbol of duration 2048 (2K) samples with sampling rate $1/T_s$. As shown in Fig. 1, the 2K samples are divided into three parts: A, B, and C.

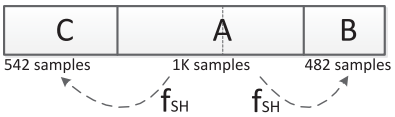

Fig. 1. Time domain structure of the P1 symbol.

The central part, denoted as part A, is generated by applying an inverse Fourier transform of size $N_a = 1024$ on the signaling vector similar to the OFDM signaling symbols in the frequency domain, where each symbol is conveyed by a distinct sub-carrier. However, as indicated in the DVB-T2 standard [1], only $M = 384$ specific sub-carriers are active when generating part A, while the other sub-carriers carry zero symbols (null carriers). Consequently, the part A signal can be written as [13]

$$\mathbf{s}_{\mathrm{A}} = \mathbf{T}_{N_a}\mathbf{P}\mathbf{d}, \tag{1}$$

where $\mathbf{d} = [d_0, d_1, \ldots, d_{M-1}]^T$ denotes the vector of signaling symbols in the frequency domain; $\mathbf{P}$ is the $N_a\times M$ active carrier pattern matrix with entries

$$[\mathbf{P}]_{n,m} = \begin{cases} 1, & \text{the } n\text{-th carrier is the } m\text{-th active carrier} \\ 0, & \text{otherwise} \end{cases}$$

for $n = 1, 2, \ldots, N_a$ and $m = 1, 2, \ldots, M$; $\mathbf{T}_{N_a}$ is the N_a-size power-normalized inverse Fourier matrix with entries $[\mathbf{T}_{N_a}]_{p,q} = e^{j2\pi(p-1)(q-1)/N_a}/\sqrt{M}$ for $p, q = 1, 2, \ldots, N_a$; $\mathbf{s}_{\mathrm{A}} = [s_{\mathrm{A}}(0), s_{\mathrm{A}}(1), \ldots, s_{\mathrm{A}}(N_a - 1)]^T$ denotes the sample vector of part A generated by a transmitter.

Parts C and B are obtained by repeating the first $N_c = 542$ samples and the last $N_b = 482$ samples of $\mathbf{s}_{\mathrm{A}}$, respectively (note $N_a = N_b + N_c$), each with a frequency shift of $f_{\mathrm{SH}} = 1/(N_a T_s)$. Let $\mathbf{T}_{N_c}$ and $\mathbf{T}_{N_b}$ be two matrices containing the first N_c and the last N_b rows of $\mathbf{T}_{N_a}$, respectively, and $\mathbf{T} = [\mathbf{T}_{N_c}^T, \mathbf{T}_{N_a}^T, \mathbf{T}_{N_b}^T]^T$; let $\mathbf{E}_{N_c}$ and $\mathbf{E}_{N_b}$ denote N_c-size and N_b-size diagonal matrices, respectively, with $[\mathbf{E}_{N_c}]_{p,p} = e^{j2\pi p/N_a}$ for $p = 0, 1, \ldots, N_c - 1$ and $[\mathbf{E}_{N_b}]_{p,p} = e^{j2\pi p/N_a}$ for $p = N_c, N_c + 1, \ldots, N_a - 1$, and

$$\mathbf{E} = \begin{bmatrix} \mathbf{E}_{N_c} & \mathbf{0}_{N_c\times N_a} & \mathbf{0}_{N_c\times N_b} \\ \mathbf{0}_{N_a\times N_c} & \mathbf{I}_{N_a} & \mathbf{0}_{N_a\times N_b} \\ \mathbf{0}_{N_b\times N_c} & \mathbf{0}_{N_b\times N_a} & \mathbf{E}_{N_b} \end{bmatrix}. \tag{2}$$

Then, the $2N_a$-size vector of the transmitted P1 symbol $\mathbf{s}_{\mathrm{P1}} = [s_{\mathrm{P1}}(0), s_{\mathrm{P1}}(1), \ldots, s_{\mathrm{P1}}(2N_a - 1)]^T$ can be written as [13]

$$\mathbf{s}_{\mathrm{P1}} = \mathbf{E}\mathbf{T}\mathbf{P}\mathbf{d}. \tag{3}$$

In the problem setup, we consider an unknown fading channel which introduces a carrier frequency offset Φ (normalized with respect to the bandwidth $1/T_s$) and a delay of τ samples. Also, we assume that the detection phase of the P1 symbol has been completed. N ($N > 2N_a$) consecutive samples of $x(n)$ are collected in a column vector (see Fig. 2) for each estimation procedure; $\mathbf{s}_1 = [s_1(0), s_1(1), \ldots, s_1(\tau - 1)]^T$

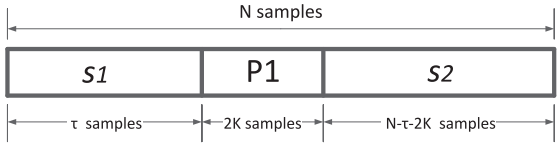

Fig. 2. Transmitted signal during the observing window.

and $\mathbf{s}_2 = [s_2(0), s_2(1), \ldots, s_2(N-\tau-2N_a-1)]^T$ are used to denote the signals transmitted before and after the P1 symbol, respectively. Hence, the observed data $\mathbf{x} = [x(0), x(1), \ldots, x(N-1)]^T$ at the receive end is given by

$$\mathbf{x} = \alpha \mathbf{s} \odot \mathbf{e} + \mathbf{w}, \tag{4}$$

where α denotes the unknown coefficient regarding the channel gain, $\mathbf{s} = [s(0), s(1), \ldots, s(N-1)]^T$ with

$$s(n) = \begin{cases} s_1(n), & n \in [0, \tau-1] \\ s_{\mathrm{P1}}(n-\tau), & n \in [\tau, \tau+2N_a-1] \\ s_2(n-\tau-2N_a), & n \in [\tau+2N_a, N-1], \end{cases} \tag{5}$$

$\mathbf{e} = [1, e^{j2\pi\Phi}, \ldots, e^{j2\pi\Phi(N-1)}]^T$ transforms the CFO onto the discrete time domain, and $\mathbf{w} = [w(0), w(1), \ldots, w(N-1)]^T$ is the noise sample vector with distribution

$$\mathbf{w} \sim \mathcal{CN}(\mathbf{0}, \eta \mathbf{I}_N), \tag{6}$$

where η is the noise power (variance). Note that τ is an integer in $[0, N-2N_a]$, and that Φ can be decomposed into an integer number ($0 \le F < N_a$) of sub-carriers plus a fractional part ($0 \le \phi < 1$) of a sub-carrier whose normalized spacing is $1/N_a$ [7], i.e.,

$$\Phi = \frac{1}{N_a}(F + \phi). \tag{7}$$

In [13], it is assumed that the total received signal power and $E\{|\alpha s(n)|^2\}$, which is the contribution from the DVB-T2 signal, are both known. Although the total received power can be measured in practice, it is not easy to estimate the power of the DVB-T2 signal, which is affected by the fading channel and contaminated by the noise, prior to synchronization. Herein, we consider a more general channel environment where the channel coefficient α is unknown.

The problem of interest is to jointly estimate the time delay τ and the CFO Φ from the observations $\{x(n)\}$ by means of ML methods. Two different approaches are developed by describing the DVB-T2 signal $\{s(n)\}$ with a stochastic and, respectively, a deterministic model.

III. Stochastic Model Based Approach

Prior to synchronization and demodulation, the symbols $\mathbf{d}$ in (3) are unknown and can be modeled as independent, identically distributed (i.i.d.) random variables with zero mean and unit variance [1], [13]. For a sufficiently large number of active carriers and using the central limit theorem, the transmitted P1 symbol $\mathbf{s}_{\mathrm{P1}}$ is approximated as zero-mean complex Gaussian distributed with covariance matrix

$$\mathbf{R} = E\{\mathbf{s}_{\mathrm{P1}}\mathbf{s}_{\mathrm{P1}}^H\} = \mathbf{E}\mathbf{T}\mathbf{P}\mathbf{P}^H\mathbf{T}^H\mathbf{E}^H. \tag{8}$$

Without the particular structure as in the P1 symbol, $\mathbf{s}_1$ and $\mathbf{s}_2$ are both considered as zero-mean complex Gaussian distributed with identity covariance matrices. Therefore, the transmitted signal $\mathbf{s} = \left[\mathbf{s}_1^T, \mathbf{s}_{\mathrm{P1}}^T, \mathbf{s}_2^T\right]^T$ can be modeled as zero-mean complex Gaussian distributed with covariance matrix

$$\mathbf{R}_s(\tau) = \begin{bmatrix} \mathbf{I}_\tau & \mathbf{0}_{\tau\times 2N_a} & \mathbf{0}_{\tau\times N'} \\ \mathbf{0}_{2N_a\times\tau} & \mathbf{R} & \mathbf{0}_{2N_a\times N'} \\ \mathbf{0}_{N'\times\tau} & \mathbf{0}_{N'\times 2N_a} & \mathbf{I}_{N'} \end{bmatrix}, \tag{9}$$

where $N' = N - \tau - 2N_a$, and the vectors $\mathbf{s}_1$, $\mathbf{s}_{\mathrm{P1}}$, $\mathbf{s}_2$ are mutually independent. Let $\mathbf{K}(\Phi)$ denote the N-size diagonal matrix with $[\mathbf{K}(\Phi)]_{p,p} = e^{j2\pi\Phi(p-1)}$ for $p = 1, 2, \ldots, N$, and $\eta_s = |\alpha|^2$. We eventually obtain

$$\mathbf{x} \sim \mathcal{CN}(\mathbf{0}, \mathbf{R}_x), \tag{10}$$

where

$$\mathbf{R}_x = \mathbf{K}(\Phi)\mathbf{Q}\mathbf{K}(\Phi)^H, \tag{11}$$

and

$$\mathbf{Q} = \eta_s \mathbf{R}_s(\tau) + \eta \mathbf{I}_N. \tag{12}$$

Next, we discuss the general case of the stochastic model based ML approach, referred to as the SML, with unknown signal power η_s and known noise power η.

A. SML

According to (10), the log-likelihood function (LLF) of the observed data $\mathbf{x}$ is

$$\begin{aligned} \Lambda(\eta_s, \tau, \Phi) &\triangleq \ln f(\mathbf{x}|\eta_s, \tau, \Phi) \\ &= -\mathbf{x}^H\mathbf{R}_x^{-1}\mathbf{x} - \ln|\mathbf{R}_x| - N\ln\pi. \end{aligned} \tag{13}$$

From (11), we have

$$\mathbf{R}_x^{-1} = \mathbf{K}(\Phi)\mathbf{Q}^{-1}\mathbf{K}(\Phi)^H, \tag{14}$$

and

$$|\mathbf{R}_x| = |\mathbf{Q}|. \tag{15}$$

From (9) and (12), we obtain

$$\mathbf{Q}^{-1} = \begin{bmatrix} \frac{1}{\eta_s+\eta}\mathbf{I}_\tau & \mathbf{0}_{\tau\times 2N_a} & \mathbf{0}_{\tau\times N'} \\ \mathbf{0}_{2N_a\times\tau} & \mathbf{B}^{-1} & \mathbf{0}_{2N_a\times N'} \\ \mathbf{0}_{N'\times\tau} & \mathbf{0}_{N'\times 2N_a} & \frac{1}{\eta_s+\eta}\mathbf{I}_{N'} \end{bmatrix}, \tag{16}$$

and

$$|\mathbf{Q}| = |\mathbf{B}|(\eta_s+\eta)^{N-2N_a}, \tag{17}$$

where

$$\mathbf{B} = \eta_s\mathbf{R} + \eta\mathbf{I}_{2N_a}. \tag{18}$$

As a result,

$$\begin{aligned} \Lambda(\eta_s, \tau, \Phi) = &-\frac{\Gamma_2(\tau)}{\eta_s+\eta} - (N-2N_a)\ln(\eta_s+\eta) - N\ln\pi \\ &- \mathbf{x}_{\mathrm{P1}}(\tau)^H\mathbf{K}_{\mathrm{P1}}(\tau,\Phi)\mathbf{B}^{-1}\mathbf{K}_{\mathrm{P1}}(\tau,\Phi)^H\mathbf{x}_{\mathrm{P1}}(\tau) \\ &- \ln|\mathbf{B}|, \end{aligned} \tag{19}$$

where $\Gamma_2(\tau) = \sum_{n=0}^{\tau-1}|x(n)|^2 + \sum_{n=\tau+2N_a}^{N-1}|x(n)|^2$, $\mathbf{x}_{\mathrm{P1}}(\tau) = [x(\tau), x(\tau+1), \ldots, x(\tau+2N_a-1)]^T$, and $\mathbf{K}_{\mathrm{P1}}(\tau, \Phi)$

denotes the $2N_a$-size diagonal matrix with $[\mathbf{K}_{\mathrm{P1}}(\tau, \Phi)]_{p,p} = e^{j2\pi\Phi(\tau+p-1)}$ for $p = 1, 2, \ldots, 2N_a$.

The ML estimation is obtained by maximizing $\Lambda(\eta_s, \tau, \Phi)$ subject to η_s, τ, and Φ. Particularly, we use the following search strategy to accomplish this task. First, for each possible integer value of τ we maximize $\Lambda(\eta_s, \tau, \Phi)$ with respect to η_s and Φ simultaneously, obtaining

$$\left(\bar{\eta_s}(\tau), \bar{\Phi}(\tau)\right) = \arg\max_{\eta_s, \Phi} \Lambda(\eta_s, \Phi|\tau). \tag{20}$$

This optimization problem (20) will be discussed in the next paragraph. Next, we find the ML estimate of τ as

$$\hat{\tau} = \arg\max_{\tau} \Lambda\left(\bar{\eta_s}(\tau), \tau, \bar{\Phi}(\tau)\right), \tag{21}$$

and consequently the ML estimates for η_s and Φ, i.e.,

$$\hat{\eta_s} = \bar{\eta_s}\left(\hat{\tau}\right) \quad \text{and} \quad \hat{\Phi} = \bar{\Phi}\left(\hat{\tau}\right). \tag{22}$$

To solve the sub-problem (20), a cyclic iteration algorithm is used. Specifically, at the k-th iteration, the k-th update of η_s is obtained by nulling the derivative of $\Lambda(\eta_s, \Phi^{(k-1)}|\tau)$ with respect to η_s, i.e.,

$$\frac{\partial \Lambda\left(\eta_s, \Phi^{(k-1)}|\tau\right)}{\partial \eta_s} = 0, \tag{23}$$

and the k-th update of Φ is given by solving the equation below,

$$\frac{\partial \Lambda\left(\eta_s^{(k)}, \Phi|\tau\right)}{\partial \Phi} = 0, \tag{24}$$

where

$$\begin{aligned}\frac{\partial \Lambda(\eta_s, \Phi|\tau)}{\partial \eta_s} = {} & \frac{\Gamma_2(\tau)}{(\eta_s+\eta)^2} - \frac{2N_aM}{2N_a\eta_s + M\eta} - \frac{N-2N_a}{\eta_s+\eta} \\ & + \Big[\mathbf{x}_{\mathrm{P1}}(\tau)^H \mathbf{K}_{\mathrm{P1}}(\tau, \Phi)\mathbf{B}^{-1}\mathbf{R}\mathbf{B}^{-1} \\ & \times \mathbf{K}_{\mathrm{P1}}(\tau, \Phi)^H \mathbf{x}_{\mathrm{P1}}(\tau)\Big],\end{aligned} \tag{25}$$

and

$$\begin{aligned}\frac{\partial \Lambda(\eta_s, \Phi|\tau)}{\partial \Phi} = {} & \mathbf{x}_{\mathrm{P1}}(\tau)^H \mathbf{K}_{\mathrm{P1}}(\tau, \Phi)\Big[\mathbf{B}^{-1}\mathbf{D}(\tau) - \mathbf{D}(\tau)\mathbf{B}^{-1}\Big] \\ & \times \mathbf{K}_{\mathrm{P1}}(\tau, \Phi)^H \mathbf{x}_{\mathrm{P1}}(\tau)\end{aligned} \tag{26}$$

with $\mathbf{D}(\tau)$ denoting the $2N_a$-size diagonal matrix whose elements $[\mathbf{D}(\tau)]_{p,p} = j2\pi(\tau+p-1)$ for $p = 1, 2, \ldots, 2N_a$. This process is repeated until the convergence is achieved.

Although the SML method can handle the general case of the problem based on the stochastic model, its computational complexity is quite high. In the following, the ML estimator is simplified by neglecting the effect of the null carriers. The derived method is referred to as the approximate SML (ASML). The performances of these two algorithms will be demonstrated in Section V.

B. ASML

By assuming that all sub-carriers are active when generating the P1 symbol, the number of signaling symbols in the frequency domain $M = N_a$ and the pattern matrix $\mathbf{P}$ can be simplified as an identity matrix $\mathbf{I}_{N_a}$. Then, we have

$$\mathbf{R} = \begin{bmatrix} \mathbf{I}_{N_c} & \mathbf{E}_{N_c} & \mathbf{0}_{N_c\times N_b} & \mathbf{0}_{N_c\times N_b} \\ \mathbf{E}_{N_c}^H & \mathbf{I}_{N_c} & \mathbf{0}_{N_c\times N_b} & \mathbf{0}_{N_c\times N_b} \\ \mathbf{0}_{N_b\times N_c} & \mathbf{0}_{N_b\times N_c} & \mathbf{I}_{N_b} & \mathbf{E}_{N_b}^H \\ \mathbf{0}_{N_b\times N_c} & \mathbf{0}_{N_b\times N_c} & \mathbf{E}_{N_b} & \mathbf{I}_{N_b} \end{bmatrix}, \tag{27}$$

which indicates that the pairwise correlation of the samples in the transmitted P1 symbol only occurs between each sample in the part A signal and its corresponding frequency-shifted repetition in part C or B. The observed data vector $\mathbf{x}$ has the same correlation property. Accordingly, we find the LLF (see Appendix A) given by

$$\begin{aligned}\Lambda(\eta_s, \tau, \Phi) = {} & \frac{2\eta_s}{\eta^2 + 2\eta\eta_s}\Upsilon(\tau, \Phi) - \frac{\eta+\eta_s}{\eta^2+2\eta\eta_s}\Gamma_1(\tau) \\ & - \frac{1}{\eta+\eta_s}\Gamma_2(\tau) - (N-2N_a)\ln(\eta+\eta_s) \\ & - N_a \ln\left(\eta^2 + 2\eta\eta_s\right) - N\ln\pi,\end{aligned} \tag{28}$$

where

$$\Gamma_1(\tau) = \sum_{n=\tau}^{\tau+2N_a-1} |x(n)|^2, \tag{29}$$

$$\Gamma_2(\tau) = \sum_{n=0}^{N-1} |x(n)|^2 - \Gamma_1(\tau), \tag{30}$$

and

$$\begin{aligned}\Upsilon(\tau, \Phi) = {} & |r_c(\tau)|\cos(2\pi\Phi N_c + \angle r_c(\tau)) \\ & + |r_b(\tau)|\cos(2\pi\Phi N_b + \angle r_b(\tau))\end{aligned} \tag{31}$$

with

$$\begin{aligned} r_c(\tau) &= |r_c(\tau)|e^{j\angle r_c(\tau)} \\ &= \sum_{n=\tau}^{\tau+N_c-1} x(n)x^*(n+N_c)e^{-j2\pi(n-\tau)/N_a}, \end{aligned} \tag{32}$$

and

$$\begin{aligned} r_b(\tau) &= |r_b(\tau)|e^{j\angle r_b(\tau)} \\ &= \sum_{n=\tau+2N_c}^{\tau+2N_c+N_b-1} x(n)x^*(n+N_b)e^{j2\pi(n-\tau-N_c)/N_a}. \end{aligned} \tag{33}$$

The ML estimates are obtained as

$$\left(\hat{\eta_s}, \hat{\tau}, \hat{\Phi}\right) = \arg\max_{\eta_s, \tau, \Phi} \Lambda(\eta_s, \tau, \Phi), \tag{34}$$

where $\Lambda(\eta_s, \tau, \Phi)$ is defined in (28). To solve this optimization problem, as previously discussed, we should first maximize (28) with respect to Φ and η_s for each value of τ. Note that given τ the only term containing Φ is $\Upsilon(\tau, \Phi)$ defined in (31). Thus,

$$\bar{\Phi}(\tau) = \arg\max_{\Phi} \Upsilon(\Phi|\tau). \tag{35}$$

Furthermore, the intermediate estimate $\bar{\eta}_s(\tau)$ of η_s can be obtained by nulling the derivative of $\Lambda(\eta_s, \bar{\Phi}(\tau)|\tau)$ with respect to η_s, i.e.,

$$\frac{\partial \Lambda\left(\eta_s, \bar{\Phi}(\tau)|\tau\right)}{\partial \eta_s} = \frac{2\Upsilon(\tau, \bar{\Phi}(\tau)) + \Gamma_1(\tau)}{(2\eta_s+\eta)^2} + \frac{\Gamma_2(\tau)}{(\eta_s+\eta)^2} - \frac{N-2N_a}{\eta_s+\eta} - \frac{2N_a}{2\eta_s+\eta} = 0. \tag{36}$$

Using the estimates $\bar{\Phi}(\tau)$ and $\bar{\eta}_s(\tau)$, we obtain the ML estimate of τ as

$$\hat{\tau} = \arg\max_{\tau} \Lambda\left(\bar{\eta}_s(\tau), \tau, \bar{\Phi}(\tau)\right). \tag{37}$$

Consequently,

$$\hat{\Phi} = \bar{\Phi}\left(\hat{\tau}\right) \quad \text{and} \quad \hat{\eta}_s = \bar{\eta}_s\left(\hat{\tau}\right). \tag{38}$$

C. Cramér–Rao Lower Bound

In this section, we consider the CRLBs of the estimated CFO $\hat{\Phi}$ and received signal power $\hat{\eta}_s$ for the stochastic model based problem. The unknown parameter vector $\boldsymbol{\theta} = [\theta_1, \theta_2]^T$ can be written as

$$\boldsymbol{\theta} = [\Phi, \eta_s]^T. \tag{39}$$

From the *Slepian-Bangs formula* [31, p. 525] and the observed data distribution (10), we obtain the 2-by-2 Fisher information matrix (FIM) $\mathbf{F}_s$ (see Appendix B) as

$$[\mathbf{F}_s]_{1,1} = -\frac{8}{3}\pi^2 N_a\left[6\tau^2 + 6(2N_a-1)\tau + 8N_a^2 - 6N_a + 1\right] - 2\,\mathrm{tr}\left\{\mathbf{B}^{-1}\mathbf{D}(\tau)\mathbf{B}\mathbf{D}(\tau)\right\}, \tag{40}$$

$$[\mathbf{F}_s]_{2,2} = \frac{4N_a^2 M}{(2N_a\eta_s + M\eta)^2} + \frac{N-2N_a}{(\eta_s+\eta)^2}, \tag{41}$$

and $[\mathbf{F}_s]_{1,2} = [\mathbf{F}_s]_{2,1} = 0$. The corresponding CRLBs for Φ and η_s are

$$\mathrm{CRLB}_{\theta_p} = \left[\mathbf{F}_s^{-1}\right]_{p,p} = \frac{1}{[\mathbf{F}_s]_{p,p}}, \text{ for } p = 1, 2. \tag{42}$$

In the absence of null carriers, the CRLBs can be further simplified as

$$\mathrm{CRLB}_{\Phi} = \frac{\eta(2\eta_s+\eta)}{8\pi^2\left(N_c^3 + N_b^3\right)\eta_s^2}, \tag{43}$$

and

$$\mathrm{CRLB}_{\eta_s} = \frac{(2\eta_s+\eta)^2(\eta_s+\eta)^2}{4N_a(\eta_s+\eta)^2 + (N-2N_a)(2\eta_s+\eta)^2}. \tag{44}$$

IV. Deterministic Model Based Approach

In this section, a new approach is developed by modeling the transmitted signal $\mathbf{s}$ as deterministic but unknown. It has the advantage of being more flexible and simpler in implementation, not requiring any stochastic model on the transmitted signal; in addition, the resulting algorithm is independent of whether null carriers are present or not.

Under the deterministic assumption for the transmitted signal, the unknown coefficient α can be absorbed into the complex-valued $\mathbf{s}$. Therefore, in this section the model for the observed data can be written as

$$\mathbf{x} = \mathbf{s} \odot \mathbf{e} + \mathbf{w} = \mathbf{K}(\Phi)\mathbf{s} + \mathbf{w}. \tag{45}$$

Due to the Gaussian assumption of $\mathbf{w}$ in (6), we have

$$\mathbf{x} \sim \mathcal{CN}(\mathbf{K}(\Phi)\mathbf{s}, \eta\mathbf{I}_N), \tag{46}$$

where $\mathbf{s}$ and η are both unknown. In the following, the deterministic model based ML approach, referred to as the DML, is presented.

A. DML

The likelihood function of $\mathbf{x}$ in the deterministic signal model is given by

$$f(\mathbf{x}|\mathbf{s}, \tau, \Phi, \eta) = \frac{1}{\pi^N\eta^N}\exp\left[-\frac{(\mathbf{x}-\mathbf{s}\odot\mathbf{e})^H(\mathbf{x}-\mathbf{s}\odot\mathbf{e})}{\eta}\right]. \tag{47}$$

Referring to the signal structure of $\mathbf{s}$ in Fig. 2 and the P1 symbol structure in Fig. 1, the LLF of the observed data $\mathbf{x}$ can be written as

$$\Lambda(\mathbf{s}, \tau, \Phi, \eta) \triangleq \ln f(\mathbf{x}|\mathbf{s}, \tau, \Phi, \eta) = -\frac{\Delta}{\eta} - N\ln\eta - N\ln\pi, \tag{48}$$

where

$$\begin{aligned}\Delta &\triangleq (\mathbf{x}-\mathbf{s}\odot\mathbf{e})^H(\mathbf{x}-\mathbf{s}\odot\mathbf{e}) \\ &= \sum_{n=0}^{\tau-1}\left|x(n) - s_1(n)e^{j2\pi\Phi n}\right|^2 \\ &\quad + \sum_{n=\tau}^{\tau+N_c-1}\left|x(n) - s_{\mathrm{A}}(n-\tau)e^{j2\pi\left(\Phi n + \frac{n-\tau}{N_a}\right)}\right|^2 \\ &\quad + \sum_{n=\tau+N_c}^{\tau+N_c+N_a-1}\left|x(n) - s_{\mathrm{A}}(n-\tau-N_c)e^{j2\pi\Phi n}\right|^2 \\ &\quad + \sum_{n=\tau+N_c+N_a}^{\tau+2N_a-1}\left|x(n) - s_{\mathrm{A}}(n-\tau-N_a)e^{j2\pi\left(\Phi n + \frac{n-\tau-N_a}{N_a}\right)}\right|^2 \\ &\quad + \sum_{n=\tau+2N_a}^{N-1}\left|x(n) - s_2(n-\tau-2N_a)e^{j2\pi\Phi n}\right|^2.\end{aligned} \tag{49}$$

Since maximizing the likelihood function $f(\mathbf{x}|\mathbf{s}, \tau, \Phi, \eta)$ is equivalent to maximizing the LLF $\Lambda(\mathbf{s}, \tau, \Phi, \eta)$, the ML estimation is

$$\left(\hat{\mathbf{s}}, \hat{\tau}, \hat{\Phi}, \hat{\eta}\right) = \arg\max_{\mathbf{s},\tau,\Phi,\eta} \Lambda(\mathbf{s}, \tau, \Phi, \eta). \tag{50}$$

From (48) and (49), it is shown that only the term Δ involves the parameters $(\mathbf{s}, \tau, \Phi)$ and its value is inversely proportional to the value of the objective function $\Lambda(\mathbf{s}, \tau, \Phi, \eta)$. Therefore, the ML estimates of $(\mathbf{s}, \tau, \Phi)$ can be determined by

$$\left(\hat{\mathbf{s}}, \hat{\tau}, \hat{\Phi}\right) = \arg\min_{\mathbf{s},\tau,\Phi} \Delta(\mathbf{s}, \tau, \Phi). \tag{51}$$

This optimization problem can be solved as follows. According to (49), we can first obtain the intermediate ML estimates of $\mathbf{s}$, given τ and Φ, as

$$\bar{s_1}(n) = x(n)e^{-j2\pi\Phi n}, \tag{52}$$

$$\bar{s_2}(n) = x(n+\tau+2N_a)e^{-j2\pi\Phi(n+\tau+2N_a)}, \tag{53}$$

$$\bar{s_A}(n) = \frac{1}{2}\Big\{x(n+\tau)e^{-j2\pi[\Phi(n+\tau)+n/N_a]} + x(n+\tau+N_c)e^{-j2\pi\Phi(n+\tau+N_c)}\Big\}, \tag{54}$$

for $n = 0, \ldots, N_c - 1$, and

$$\bar{s_A}(n) = \frac{1}{2}\Big\{x(n+\tau+N_c)e^{-j2\pi\Phi(n+\tau+N_c)} + x(n+\tau+N_a)e^{-j2\pi[\Phi(n+\tau+N_a)+n/N_a]}\Big\}, \tag{55}$$

for $n = N_c, \ldots, N_a - 1$. Substituting the above results back into (49), Δ becomes a function of two unknown variables τ and Φ, i.e.,

$$\Delta(\tau, \Phi) = \frac{1}{2}\Gamma_1(\tau) - \Upsilon(\tau, \Phi), \tag{56}$$

where $\Gamma_1(\tau)$ and $\Upsilon(\tau, \Phi)$ are defined in (29) and (31), respectively. Then, we use the following two-dimensional search method to minimize $\Delta(\tau, \Phi)$ subject to τ and Φ. First, for each value of τ we minimize $\Delta(\tau, \Phi)$ with respect to Φ, obtaining

$$\begin{aligned}\bar{\Phi}(\tau) &= \arg\min_{\Phi} \Delta(\Phi|\tau) \\ &= \arg\max_{\Phi} \Upsilon(\Phi|\tau),\end{aligned} \tag{57}$$

where the second equivalent stems from the fact that the $\Gamma_1(\tau)$ term in (56) can be neglected in this phase when τ is given. Second, we find the time delay that minimizes $\Delta(\tau, \Phi)$, i.e.,

$$\hat{\tau} = \arg\min_{\tau} \Delta\big(\tau, \bar{\Phi}(\tau)\big). \tag{58}$$

Consequently,

$$\hat{\Phi} = \bar{\Phi}\big(\hat{\tau}\big). \tag{59}$$

The ML estimates $\hat{\mathbf{s}}$ is obtained by replacing (τ, Φ) with $(\hat{\tau}, \hat{\Phi})$ in (52)–(55). Additionally, the ML estimate of the nuisance parameter η is given by

$$\hat{\eta} = \frac{\Delta\Big(\hat{\mathbf{s}}, \hat{\tau}, \hat{\Phi}\Big)}{N}. \tag{60}$$

B. Cramér–Rao Lower Bound

The CRLB of $\hat{\Phi}$ for the deterministic model based problem is considered in this section. According to the above analysis of the DML, the unknown parameter vector can be written as

$$\begin{aligned}\boldsymbol{\xi} &= \big[\xi_0, \xi_1, \ldots, \xi_{2N-2N_a+1}\big]^T \\ &= \big[\Phi, \mathbf{s}_{1,\mathrm{re}}^T, \mathbf{s}_{\mathrm{A},\mathrm{re}}^T, \mathbf{s}_{2,\mathrm{re}}^T, \mathbf{s}_{1,\mathrm{im}}^T, \mathbf{s}_{\mathrm{A},\mathrm{im}}^T, \mathbf{s}_{2,\mathrm{im}}^T, \eta\big]^T,\end{aligned} \tag{61}$$

where $\mathbf{s}_{\star,\mathrm{re}} = \Re\{\mathbf{s}_\star\}$ and $\mathbf{s}_{\star,\mathrm{im}} = \Im\{\mathbf{s}_\star\}$. From the Slepian-Bangs formula and the observed data distribution (46), the FIM $\mathbf{F}_d$ with dimension $2N-2N_a+2$ is obtained (see Appendix C). By treating $\mathbf{F}_d$ as a block matrix

$$\begin{bmatrix} r & \mathbf{v}^T \\ \mathbf{v} & \mathbf{G} \end{bmatrix}$$

TABLE I
PARAMETERS USED IN SIMULATIONS

$N = 6N_a$	M	ϕ	Φ	τ	η
6144	384	0.45	$\frac{0.45}{1024}$	100	1

with

$$\begin{aligned} r &= [\mathbf{F}_d]_{1,1}, \\ \mathbf{v} &= \mathbf{F}_d(2 : 2N - 2N_a + 2, 1), \\ \mathbf{G} &= \mathbf{F}_d(2 : 2N - 2N_a + 2, 2 : 2N - 2N_a + 2), \end{aligned}$$

the CRLB for the estimated CFO $\hat{\Phi}$ in the deterministic model based problem is

$$\mathrm{CRLB}_\Phi = \Big(r - \mathbf{v}^T\mathbf{G}^{-1}\mathbf{v}\Big)^{-1}. \tag{62}$$

Note that $\mathbf{G}$ is a diagonal matrix. The CRLB for the estimated noise power $\hat{\eta}$ can also be obtained as

$$\mathrm{CRLB}_\eta = \frac{\eta^2}{N}. \tag{63}$$

V. SIMULATION RESULTS

In this section, we present numerical results to compare the performances of the proposed SML, ASML, and DML algorithms, as well as the CC algorithm [6] and the method [13] which is referred to as the RTV method. Note that the RTV method assumes the knowledge of the DVB-T2 signal power, which is not required by the other methods. The observed DVB-T2 data used in the simulations is generated according to Section II. The system parameters are shown in Table I, and the active carrier pattern can be found in [1]. The definition of signal-to-noise ratio (SNR) is given by

$$\mathrm{SNR} = \frac{|\alpha|^2}{\eta}. \tag{64}$$

Figs. 3–5(a) compare the estimation performance in terms of mean squared error (MSE) defined as

$$\mathrm{MSE} = E\Big\{\big|\hat{p} - p_0\big|^2\Big\}, \tag{65}$$

where $\hat{p}$ and p_0 are the estimated and the actual values of the intended parameter, respectively, and 1000 Monte Carlo trials are conducted for the expectation operation.

Fig. 3 shows the performance of time delay estimation for the five schemes. We can see that all proposed methods outperform the CC method, and the gain is significant especially in the region of high SNR. The SML method has the lowest MSE among all methods, due to the fact that the SML exploits the null-carrier structure of the P1 symbol for estimation, but the others do not. The benefit also comes with a significant computational cost as shown later. It is interesting to see that the proposed ASML and DML methods achieve the same performance as the RTV method, without requiring the knowledge of the DVB-T2 signal power. Hence, there is no performance loss in including the signal power parameter in the joint estimation problem.

The performance of CFO estimation is shown in Fig. 4. We observe that the proposed methods outperform the CC method.

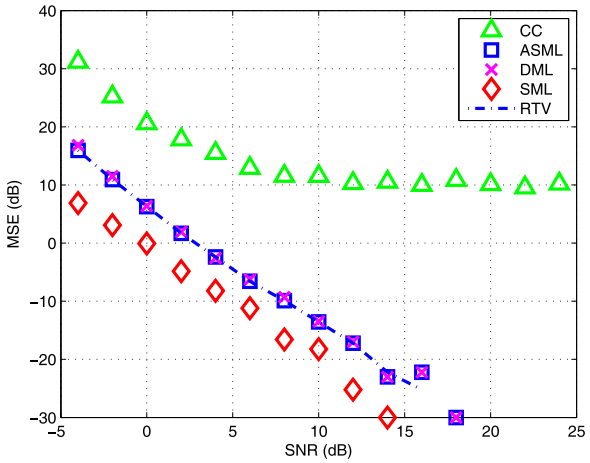

Fig. 3. Performance of time delay estimation.

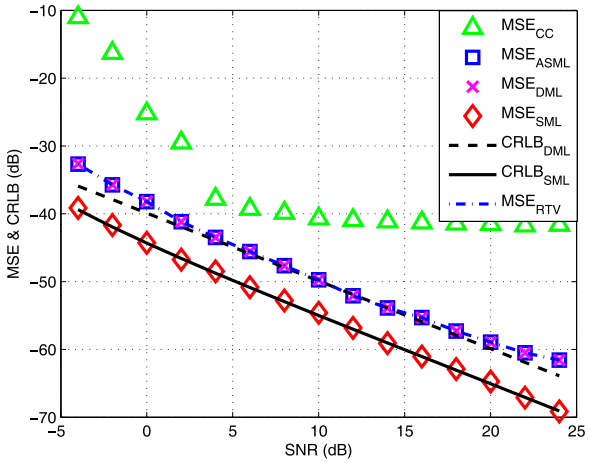

Fig. 4. Performance of CFO estimation.

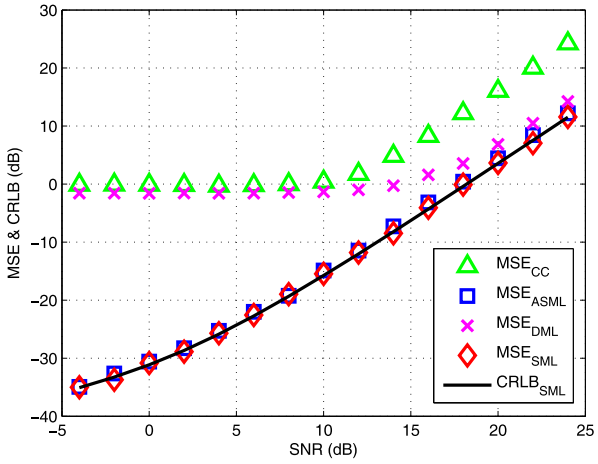

(a)

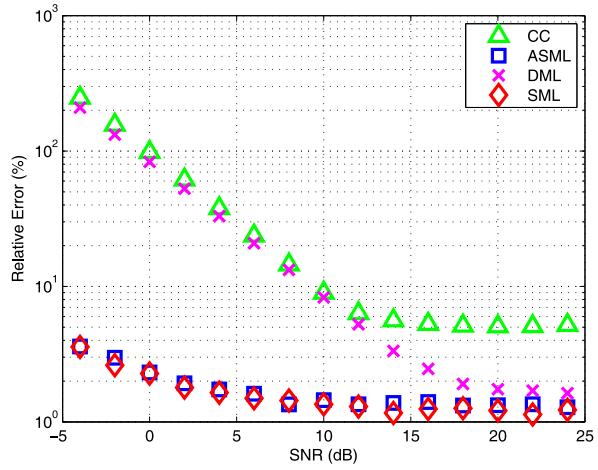

(b)

Fig. 5. Performance of signal power estimation. (a) MSE; (b) relative error.

Again, the performances of ASML, DML, and RTV coincide with each other. In addition, the SML method has the best performance for CFO estimation. For comparison purposes, the CRLBs for CFO estimation are also included. It is shown that the MSE curves of SML and DML are very close to the CRLB curves for the stochastic and deterministic model based problems, respectively.

The MSEs of signal power estimates for different estimators, as well as the CRLB based on the stochastic model, are presented in Fig. 5(a). It is worth mentioning that DML does not provide a direct estimate of the signal power. Here, an indirect estimate of the power is obtained by using averaging over the estimated signal samples in (52)–(55). Since the RTV method assumes that the signal power is known, it is not included here. It is shown that the proposed approaches still outperform the CC method, but the gain of the DML over the CC method is negligible in the low SNR region. We can see that the performances of SML and ASML are similar and are quite close to the CRLB. Unlike the previous cases, the MSE curves in Fig. 5(a) have an ascending trend, since the actual received signal power increases SNR for a given noise power. To explicitly show that the estimation accuracy increases as SNR increases, Fig. 5(b) shows the performance of the received signal power estimation in terms of the relative error (RE) defined as

$$\mathrm{RE} = \frac{E\{|\hat{p} - p_0|\}}{|p_0|} \times 100\%. \tag{66}$$

The relationship among the performances of these methods observed from Fig. 5(b) is consistent with that from Fig. 5(a).

Finally, we consider the computational complexity of the CC, RTV, ASML, DML, and SML methods, which affects their required time for synchronization. The complexity is measured by the *elapsed time* in Matlab, using a PC running Matlab R2013b in Windows 7 Professional (64-bit) with 3.30 GHz CPU and 8 GB RAM. Note that all these methods employ a sliding window and estimate the delay by a sample-by-sample search process. Here, the elapsed time per sample incurred by each of the considered methods is shown in Table II. It is seen that the SML method is significantly more involved than the others, due to the cyclic iteration procedure used to find the solution. The CC method is computationally most efficient, while the remaining methods are similar to each other, with RTV being slightly faster than ASML and DML.

TABLE II
ELAPSED TIME COMPARISON

Algorithm	ms/sample
CC	0.02276
RTV	0.8889
ASML	1.626
DML	0.9181
SML	1154

VI. CONCLUSION

In this paper, new ML synchronization algorithms for DVB-T2 transmissions have been derived by modeling the transmitted signal as stochastic and, respectively, unknown deterministic. An unknown fading channel is considered in the model. The proposed SML algorithm can jointly estimate the received signal power, time delay, and CFO. By neglecting the effect of null carriers, the SML is simplified to the ASML with a lower computing complexity. On the other hand, the DML is developed based on a deterministic model. Compared with its counterparts based on the stochastic model, the DML algorithm is more flexible and has a lower complexity, at the cost of reduced estimation accuracy. Numerical results indicate that all proposed methods outperform the cross-correlation based method. The performances of the proposed ASML and DML methods are very similar to that of the RTV method which assumes knowledge of the signal power. This implies that there is no loss of accuracy by including the signal power parameter in the joint estimation problem. Although the ASML is more complex than the RTV, the complexity of the DML is similar to that of the RTV. Additionally, we observed that the CRLBs for the stochastic and the deterministic models can be achieved by the SML and the DML, respectively.

APPENDIX A
PROOF OF (28)

The likelihood function in the simplified case can be written as

$$f(\mathbf{x}|\eta_s,\tau,\Phi)=\prod_{n=0}^{\tau-1}f(x(n))\prod_{n=\tau}^{\tau+N_c-1}f(x(n),x(n+N_c))\times\prod_{n=\tau+2N_c}^{\tau+2N_c+N_b-1}f(x(n),x(n+N_b))\times\prod_{n=\tau+2N_a}^{N-1}f(x(n)),\quad(67)$$

where $f(x(n))$ for $n=0,\ldots,\tau-1$ or $\tau+2N_a,\ldots,N-1$ is given by

$$f(x(n))=\frac{1}{\pi(\eta_s+\eta)}\exp\left[-\frac{|x(n)|^2}{\eta_s+\eta}\right].\quad(68)$$

The remaining terms $f(x(n),x(n+N_i))$ for $i=c,b$ are two-dimensional zero-mean complex Gaussian distributions with covariance matrices

$$\begin{bmatrix}\eta_s+\eta & \eta_s e^{j2\pi(n'-\Phi N_c)}\\ \eta_s e^{j2\pi(\Phi N_c-n')} & \eta_s+\eta\end{bmatrix}\text{ for } i=c,\quad(69)$$

$$\begin{bmatrix}\eta_s+\eta & \eta_s e^{-j2\pi(\Phi N_b+n'')}\\ \eta_s e^{j2\pi(\Phi N_b+n'')} & \eta_s+\eta\end{bmatrix}\text{ for } i=b,\quad(70)$$

where $n'=(n-\tau)/N_a$ and $n''=(n-\tau-N_c)/N_a$. Hence, we have

$$f(x(n),x(n+N_c))=\frac{1}{\pi^2\left(\eta^2+2\eta\eta_s\right)}\times\exp\left[\frac{2\eta_s\Re\left\{x(n)x^*(n+N_c)e^{j2\pi(\Phi N_c-n')}\right\}}{\eta^2+2\eta\eta_s}-\frac{(\eta_s+\eta)\left(|x(n)|^2+|x(n+N_c)|^2\right)}{\eta^2+2\eta\eta_s}\right],\quad(71)$$

and

$$f(x(n),x(n+N_b))=\frac{1}{\pi^2\left(\eta^2+2\eta\eta_s\right)}\times\exp\left[\frac{2\eta_s\Re\left\{x(n)x^*(n+N_b)e^{j2\pi(\Phi N_b+n'')}\right\}}{\eta^2+2\eta\eta_s}-\frac{(\eta_s+\eta)\left(|x(n)|^2+|x(n+N_b)|^2\right)}{\eta^2+2\eta\eta_s}\right].\quad(72)$$

Substituting (68), (71), and (72) back into (67) and taking the natural logarithm, we get the LLF as (28).

APPENDIX B
FIM FOR THE STOCHASTIC MODEL

From (11), we get

$$\frac{\partial\mathbf{R}_x}{\partial\Phi}=\mathbf{K}(\Phi)\mathbf{C}\mathbf{Q}\mathbf{K}(\Phi)^H-\mathbf{K}(\Phi)\mathbf{Q}\mathbf{C}\mathbf{K}(\Phi)^H,\quad(73)$$

and

$$\frac{\partial\mathbf{R}_x}{\partial\eta_s}=\mathbf{K}(\Phi)\mathbf{R}_s(\tau)\mathbf{K}(\Phi)^H,\quad(74)$$

where $\mathbf{C}$ denotes the N-size diagonal matrix with $[\mathbf{C}]_{p,p}=j2\pi(p-1)$ for $p=1,2,\ldots,N$. Thus, the $(1,1)$th element of the FIM is

$$\begin{aligned}[\mathbf{F}_s]_{1,1}&=\mathrm{tr}\left\{\mathbf{R}_x^{-1}\frac{\partial\mathbf{R}_x}{\partial\Phi}\mathbf{R}_x^{-1}\frac{\partial\mathbf{R}_x}{\partial\Phi}\right\}\\&=2\,\mathrm{tr}\left\{\mathbf{C}^2-\mathbf{Q}^{-1}\mathbf{C}\mathbf{Q}\mathbf{C}\right\}\\&=2\,\mathrm{tr}\left\{\mathbf{D}(\tau)^2-\mathbf{B}^{-1}\mathbf{D}(\tau)\mathbf{B}\mathbf{D}(\tau)\right\}.\end{aligned}\quad(75)$$

By noting that $\mathrm{tr}\{\mathbf{D}(\tau)^2\}=-4\pi^2\sum_{p=\tau}^{\tau+2N_a-1}p^2$, we have (40). The $(2,2)$th element of the FIM is obtained as

$$\begin{aligned}[\mathbf{F}_s]_{2,2}&=\mathrm{tr}\left\{\mathbf{R}_x^{-1}\frac{\partial\mathbf{R}_x}{\partial\eta_s}\mathbf{R}_x^{-1}\frac{\partial\mathbf{R}_x}{\partial\eta_s}\right\}\\&=\mathrm{tr}\left\{\mathbf{Q}^{-1}\mathbf{R}_s(\tau)\mathbf{Q}^{-1}\mathbf{R}_s(\tau)\right\}\\&=\frac{N-2N_a}{(\eta_s+\eta)^2}+\mathrm{tr}\left\{\mathbf{B}^{-1}\mathbf{R}\mathbf{B}^{-1}\mathbf{R}\right\}.\end{aligned}\quad(76)$$

From (8), we find that $\mathbf{R}$ has M non-zero eigenvalues which are equal to $2N_a/M$. The matrix $\mathbf{B}^{-1}$ has the same eigenvectors as $\mathbf{R}$'s, and M of its eigenvalues are given by $M/(2N_a\eta_s+M\eta)$ and the remainder $2N_a - M$ are given by $1/\eta$. Through the relationship between the trace and the eigenvalues, we get (41). The (1, 2)th and the (2, 1)th elements of the FIM are given by

$$\begin{aligned}[\mathbf{F}_s]_{1,2} = [\mathbf{F}_s]_{2,1} &= \mathrm{tr}\left\{\mathbf{R}_x^{-1}\frac{\partial \mathbf{R}_x}{\partial \Phi}\mathbf{R}_x^{-1}\frac{\partial \mathbf{R}_x}{\partial \eta_s}\right\} \\ &= \mathrm{tr}\left\{\mathbf{Q}^{-1}\mathbf{C}\mathbf{R}_s(\tau) - \mathbf{C}\mathbf{Q}^{-1}\mathbf{R}_s(\tau)\right\} \\ &= \mathrm{tr}\left\{\mathbf{R}\mathbf{B}^{-1}\mathbf{D}(\tau) - \mathbf{B}^{-1}\mathbf{R}\mathbf{D}(\tau)\right\}. \quad (77)\end{aligned}$$

Again, through the eigen-decomposition of $\mathbf{R}$ and $\mathbf{B}^{-1}$, we find $\mathbf{R}\mathbf{B}^{-1} = \mathbf{B}^{-1}\mathbf{R}$. Hence, $[\mathbf{F}_s]_{1,2} = [\mathbf{F}_s]_{2,1} = 0$.

For the simplified case, the FIM $\mathbf{F}_s$ is

$$\mathbf{F}_s = \begin{bmatrix} -E\left\{\frac{\partial^2 \Lambda(\eta_s,\tau,\Phi)}{\partial \Phi^2}\right\} & -E\left\{\frac{\partial^2 \Lambda(\eta_s,\tau,\Phi)}{\partial \Phi \partial \eta_s}\right\} \\ -E\left\{\frac{\partial^2 \Lambda(\eta_s,\tau,\Phi)}{\partial \eta_s \partial \Phi}\right\} & -E\left\{\frac{\partial^2 \Lambda(\eta_s,\tau,\Phi)}{\partial \eta_s^2}\right\} \end{bmatrix}, \quad (78)$$

where the expectation is taken with respect to the observed data $\mathbf{x}$, and $\Lambda(\eta_s, \tau, \Phi)$ is defined in (28). By using the following results

$$\begin{aligned} E\{r_c(\tau)\} &= N_c\eta_s e^{-j2\pi\Phi N_c}, \\ E\{r_b(\tau)\} &= N_b\eta_s e^{-j2\pi\Phi N_b}, \\ E\{\Gamma_1(\tau)\} &= 2N_a(\eta_s+\eta), \\ E\{\Gamma_2(\tau)\} &= (N-2N_a)(\eta_s+\eta), \end{aligned}$$

we obtain

$$-E\left\{\frac{\partial^2 \Lambda(\eta_s,\tau,\Phi)}{\partial \Phi^2}\right\} = \frac{8\pi^2\left(N_c^3+N_b^3\right)\eta_s^2}{\eta(2\eta_s+\eta)}, \quad (79)$$

$$-E\left\{\frac{\partial^2 \Lambda(\eta_s,\tau,\Phi)}{\partial \eta_s^2}\right\} = \frac{4N_a}{(2\eta_s+\eta)^2} + \frac{N-2N_a}{(\eta_s+\eta)^2}, \quad (80)$$

$$-E\left\{\frac{\partial^2 \Lambda(\eta_s,\tau,\Phi)}{\partial \Phi \partial \eta_s}\right\} = -E\left\{\frac{\partial^2 \Lambda(\eta_s,\tau,\Phi)}{\partial \eta_s \partial \Phi}\right\} = 0. \quad (81)$$

Thus, the CRLBs of $\hat{\Phi}$ and $\hat{\eta_s}$ for the simplified case are given by (43) and (44), respectively.

APPENDIX C
FIM FOR THE DETERMINISTIC MODEL

In the distribution (46), the expectation of $\mathbf{x}$ is taken with respect to $\mathbf{s}$, τ, and Φ, while the covariance matrix $\eta\mathbf{I}_N$ only involves the unknown parameter η. Let the matrix $\mathbf{S}$ denote $\mathbf{F}_d(2 : 2N - 2N_a + 1, 2 : 2N - 2N_a + 1)$ which only contains the Fisher information of the parameters regarding the received signal $\mathbf{s}$. As a result,

$$[\mathbf{S}]_{p,q} = \frac{2}{\eta}\Re\left\{\left(\frac{\partial \mathbf{s}}{\partial \xi_p}\right)^H\left(\frac{\partial \mathbf{s}}{\partial \xi_q}\right)\right\}, \quad (82)$$

for $p, q = 1, 2, \ldots, 2N - 2N_a$. Following the results

$$\frac{\partial \mathbf{s}}{\partial \xi_p} = \begin{cases} [\mathbf{0}_{1\times p-1}, 1, \mathbf{0}_{1\times N-p}]^T, \\ \qquad \text{for } p \in [1, \tau] \\ \left[\mathbf{0}_{1\times p-1}, e^{j2\pi\frac{p-\tau-1}{N_a}}, \mathbf{0}_{1\times N_c-1}, 1, \mathbf{0}_{1\times N-N_c-p}\right]^T, \\ \qquad \text{for } p \in [\tau+1, \tau+N_c] \\ \left[\mathbf{0}_{1\times p+N_c-1}, 1, \mathbf{0}_{1\times N_b-1}, e^{j2\pi\frac{p-\tau-1}{N_a}}, \mathbf{0}_{1\times N-N_a-p}\right]^T, \\ \qquad \text{for } p \in [\tau+N_c+1, \tau+N_a] \\ \left[\mathbf{0}_{1\times p+N_a-1}, 1, \mathbf{0}_{1\times N-N_a-p}\right]^T, \\ \qquad \text{for } p \in [\tau+N_a+1, N-N_a] \end{cases}$$

and

$$\frac{\partial \mathbf{s}}{\partial \xi_p} = j\frac{\partial \mathbf{s}}{\partial \xi_{p-N+N_a}}, \text{ for } p \in [N-N_a+1, 2N-2N_a],$$

$\mathbf{S}$ is shown to be a diagonal matrix with

$$[\mathbf{S}]_{p,p} = \begin{cases} 4/\eta, & p \in [\tau+1, \tau+N_a] \\ & \quad \text{or } [\tau+N-N_a+1, \tau+N] \\ 2/\eta, & \text{otherwise.} \end{cases} \quad (83)$$

The remainder of the entries in $\mathbf{F}_d$ are calculated as follows:

$$[\mathbf{F}_d]_{1,1} = -\frac{2}{\eta}\mathbf{s}^H\mathbf{C}^2\mathbf{s}, \quad (84)$$

and

$$[\mathbf{F}_d]_{1,q} = [\mathbf{F}_d]_{q,1} = \frac{2}{\eta}\Re\left\{\mathbf{s}^H\mathbf{C}^H\frac{\partial \mathbf{s}}{\partial \xi_{q-1}}\right\}, \quad (85)$$

for $q = 2, 3, \ldots, 2N-2N_a+1$, where the matrix $\mathbf{C}$ is defined in Appendix B;

$$\begin{aligned}[\mathbf{F}_d]_{N'',N''} &= \mathrm{tr}\left\{(\eta\mathbf{I}_N)^{-1}\frac{\partial(\eta\mathbf{I}_N)}{\partial\eta}(\eta\mathbf{I}_N)^{-1}\frac{\partial(\eta\mathbf{I}_N)}{\partial\eta}\right\} \\ &= \frac{N}{\eta^2}, \quad (86)\end{aligned}$$

and

$$[\mathbf{F}_d]_{p,N''} = [\mathbf{F}_d]_{N'',p} = 0, \quad (87)$$

for $p = 1, 2, \ldots, 2N - 2N_a + 1$, where $N'' = 2N - 2N_a + 2$.

REFERENCES

[1] Eur. Telecommun. Stand. Inst., "Digital video broadcasting (DVB): Frame structure channel coding and modulation for a second generation digital terrestrial television broadcasting system (DVB-T2)," Sophia Antipolis Cedex, France, Tech. Rep. ETSI-EN-302-755-V1.1.1, Sep. 2009.

[2] Eur. Telecommun. Stand. Inst., "Digital video broadcasting (DVB): Framing structure, channel coding and modulation for digital terrestrial television," Sophia Antipolis Cedex, France, Tech. Rep. ETSI-EN-300-744-V1.5.1, Jun. 2004.

[3] J. A. C. Bingham, "Multicarrier modulation for data transmission: An idea whose time has come," *IEEE Commun. Mag.*, vol. 28, no. 5, pp. 5–14, May 1990.

[4] J.-S. Baek and J.-S. Seo, "Effective symbol timing recovery based on pilot-aided channel estimation for MISO transmission mode of DVB-T2 system," *IEEE Trans. Broadcast.*, vol. 56, no. 2, pp. 193–200, Feb. 2010.

[5] A. Viemann *et al.*, "Implementation-friendly synchronisation algorithm for DVB-T2," *Electron. Lett.*, vol. 46, no. 4, pp. 282–283, Feb. 2010.

[6] J. G. Doblado, V. Baena, A. C. Oria, D. Pérez-Calderón, and P. López, "Coarse time synchronisation for DVB-T2," *Electron. Lett.*, vol. 46, no. 11, pp. 797–799, May 2010.

[7] L. He, Z. Wang, F. Yang, S. Chen, and L. Hanzo, "Preamble design using embedded signaling for OFDM broadcast systems based on reduced-complexity distance detection," *IEEE Trans. Veh. Technol.*, vol. 60, no. 3, pp. 1217–1222, Mar. 2011.
[8] J.-S. Baek and J.-S. Seo, "Improved CIR-based receiver design for DVB-T2 system in large delay spread channels: Synchronization and equalization," *IEEE Trans. Broadcast.*, vol. 57, no. 1, pp. 103–113, Mar. 2011.
[9] C.-S. Ni, P.-J. Shih, and S.-S. Cheng, "Channel estimation and symbol boundary detection in DVB-T2 system," in *Proc. Int. Symp. VLSI Design Autom. Test (VLSI-DAT)*, Hsinchu, Taiwan, Apr. 2011, pp. 1–4.
[10] M. Yu and P. Sadeghi, "Time domain synchronization and decoding of P1 symbol in DVB-T2," in *Proc. IEEE Int. Conf. Acoust. Speech Signal Process.*, Prague, Czech Republic, May 2011, pp. 3520–3523.
[11] D. Gozalvez, D. Gomez-Barquero, D. Vargas, and N. Cardona, "Time diversity in mobile DVB-T2 systems," *IEEE Trans. Broadcast.*, vol. 57, no. 3, pp. 617–628, Sep. 2011.
[12] L. Cai, "Channel estimation using P1 symbol for DVB-T2," in *Proc. Comput. Commun. Appl. Conf. (ComComAp)*, Hong Kong, Jan. 2012, pp. 184–186.
[13] M. Rotoloni, S. Tomasin, and L. Vangelista, "Maximum likelihood estimation of time and carrier frequency offset for DVB-T2," *IEEE Trans. Broadcast.*, vol. 58, no. 1, pp. 77–86, Mar. 2012.
[14] M. Yu and P. Sadeghi, "A study of pilot-assisted OFDM channel estimation methods with improvements for DVB-T2," *IEEE Trans. Veh. Technol.*, vol. 61, no. 5, pp. 2400–2405, Jun. 2012.
[15] L. Yang, G. Ren, W. Zhai, and Z. Qiu, "Beamforming based receiver scheme for DVB-T2 system in high speed train environment," *IEEE Trans. Broadcast.*, vol. 59, no. 1, pp. 146–154, Mar. 2013.
[16] L. Vangelista and M. Rotoloni, "On the analysis of P1 symbol performance for DVB-T2," in *Proc. IEEE Sarnoff Symp.*, Princeton, NJ, USA, 2009, pp. 1–5.
[17] M. Rotoloni, S. Tomasin, and L. Vangelista, "On correlation-based synchronization for DVB-T2," *IEEE Commun. Lett.*, vol. 14, no. 3, pp. 248–250, Mar. 2010.
[18] S. Cazalens, G. Lesthievent, B. Ros, and C. Boustie, "Theoretical study of P1 detection (synchronisation for DVB-T2 standard)," in *Proc. 36th Int. Conf. Telecommun. Signal Process. (TSP)*, Rome, Italy, Jul. 2013, pp. 249–253.
[19] Eur. Telecommun. Stand. Inst., "Digital video broadcasting (DVB): Implementation guidelines for a second generation digital terrestrial television broadcasting system (DVB-T2)," Sophia Antipolis Cedex, France, Tech. Rep. ETSI-TS-102-831-V1.2.1, Aug. 2012.
[20] T. M. Schmidl and D. C. Cox, "Robust frequency and timing synchronization for OFDM," *IEEE Trans. Commun.*, vol. 45, no. 12, pp. 1613–1621, Dec. 1997.
[21] J.-J. van de Beek *et al.*, "A time and frequency synchronization scheme for multiuser OFDM," *IEEE J. Sel. Areas Commun.*, vol. 17, no. 11, pp. 1900–1914, Nov. 1999.
[22] B. Park, H. Cheon, E. Ko, C. Kang, and D. Hong, "A blind OFDM synchronization algorithm based on cyclic correlation," *IEEE Signal Process. Lett.*, vol. 11, no. 2, pp. 83–85, Feb. 2004.
[23] M. Morelli, C.-C. J. Kuo, and M.-O. Pun, "Synchronization techniques for orthogonal frequency division multiple access (OFDMA): A tutorial review," *Proc. IEEE*, vol. 95, no. 7, pp. 1394–1427, Jul. 2007.
[24] M. Morelli and M. Moretti, "Joint maximum likelihood estimation of CFO, noise power, and SNR in OFDM systems," *IEEE Wireless Commun. Lett.*, vol. 2, no. 1, pp. 42–45, Feb. 2013.
[25] A. A. M. Al-Bassiouni, M. Ismail, and W. Zhuang, "An eigenvalue based carrier frequency offset estimator for OFDM systems," *IEEE Wireless Commun. Lett.*, vol. 2, no. 5, pp. 475–478, Oct. 2013.
[26] J.-J. van de Beek, M. Sandell, and P. O. Börjesson, "ML estimation of time and frequency offset in OFDM systems," *IEEE Trans. Signal Process.*, vol. 45, no. 7, pp. 1800–1805, Jul. 1997.
[27] H. Liu and U. Tureli, "A high-efficiency carrier estimator for OFDM communications," *IEEE Commun. Lett.*, vol. 2, no. 4, pp. 104–106, Apr. 1998.
[28] X. Ma, C. Tepedelenlioglu, G. B. Giannakis, and S. Barbarossa, "Non-data-aided carrier offset estimators for OFDM with null subcarriers: Identifiability, algorithms, and performance," *IEEE J. Sel. Areas Commun.*, vol. 19, no. 12, pp. 2504–2515, Dec. 2001.
[29] Y.-S. Choi, P. J. Voltz, and F. A. Cassara, "ML estimation of carrier frequency offset for multicarrier signals in Rayleigh fading channels," *IEEE Trans. Veh. Technol.*, vol. 50, no. 2, pp. 644–655, Mar. 2001.
[30] T. S. Rappaport, *Wireless Communications: Principles and Practice*. Upper Saddle River, NJ, USA: Prentice Hall, 1996.
[31] S. M. Kay, *Fundamentals of Statistical Signal Processing: Estimation Theory*. Upper Saddle River, NJ, USA: Prentice Hall, 1993.

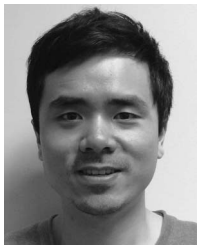

Xin Zhang received the B.Eng. degree (Hons.) from the University of Science and Technology Beijing, China, in 2008, and the M.Eng. degree from the Beijing University of Posts and Telecommunications, China, in 2011. He is currently pursuing the Ph.D. degree with the Stevens Institute of Technology, Hoboken, NJ, USA, all in electrical engineering.

Since 2013, he has been a Research and Teaching Assistant with the Department of Electrical and Computer Engineering, Stevens Institute of Technology. His research interests include statistical signal processing, optimization algorithms, passive sensing, and multichannel signal processing.

Jun Liu (S'11–M'13) received the B.S. degree in mathematics from the Wuhan University of Technology, China, in 2006, the M.S. degree in mathematics from the Chinese Academy of Sciences, China, in 2009, and the Ph.D. degree in electrical engineering from Xidian University, China, in 2012.

In 2012, he was a Post-Doctoral Research Associate with the Department of Electrical and Computer Engineering, Duke University, Durham, NC, USA, for six months. From 2013 to 2014, he was a Post-Doctoral Research Associate with the Department of Electrical and Computer Engineering, Stevens Institute of Technology, Hoboken, NJ, USA. He is currently with the National Laboratory of Radar Signal Processing, Xidian University, where he is an Associate Professor. His research interests include statistical signal processing, optimization algorithms, passive sensing, and multistatic radar.

Hongbin Li (M'99–SM'08) received the B.S. and M.S. degrees from the University of Electronic Science and Technology of China, in 1991 and 1994, respectively, and the Ph.D. degree from the University of Florida, Gainesville, FL, USA, in 1999, all in electrical engineering.

From 1996 to 1999, he was a Research Assistant with the Department of Electrical and Computer Engineering, University of Florida. Since 1999, he has been with the Department of Electrical and Computer Engineering, Stevens Institute of Technology, Hoboken, NJ, USA, where he became a Professor in 2010. He was a Summer Visiting Faculty Member with the Air Force Research Laboratory in 2003, 2004, and 2009. His general research interests include statistical signal processing, wireless communications, and radars.

Dr. Li was a recipient of the IEEE Jack Neubauer Memorial Award in 2013 from the IEEE Vehicular Technology Society, the Outstanding Paper Award from the IEEE AFICON Conference in 2011, the Harvey N. Davis Teaching Award in 2003 and the Jess H. Davis Memorial Award for excellence in research in 2001 from the Stevens Institute of Technology, and the Sigma Xi Graduate Research Award from the University of Florida in 1999. He was an Associate Editor of *Signal Processing* (Elsevier), the IEEE TRANSACTIONS ON SIGNAL PROCESSING, the IEEE SIGNAL PROCESSING LETTERS, and the IEEE TRANSACTIONS ON WIRELESS COMMUNICATIONS, a Guest Editor of the IEEE JOURNAL OF SELECTED TOPICS IN SIGNAL PROCESSING, and the *EURASIP Journal on Applied Signal Processing*, and a member of the IEEE SPS Signal Processing Theory and Methods Technical Committee (TC) and the IEEE SPS Sensor Array and Multichannel TC. He has been involved in various conference organization activities, including the General Co-Chair of the 7th IEEE Sensor Array and Multichannel Signal Processing Workshop, Hoboken, in 2012. He is a member of Tau Beta Pi and Phi Kappa Phi.

Braham Himed received the Engineer degree from the Ecole Nationale Polytechnique of Algiers in 1984, and the M.S. and Ph.D. degrees from Syracuse University, Syracuse, NY, USA, in 1987 and 1990, respectively, all in electrical engineering. He is a Technical Advisor with the Air Force Research Laboratory, Sensors Directorate, RF Technology Branch, Dayton, OH, USA, where he is involved with several aspects of radar developments. His research interests include detection, estimation, multichannel adaptive signal processing, time series analyses, array processing, adaptive processing, waveform diversity, MIMO, passive radar, and over the horizon radar. He was a recipient of the 2001 IEEE Region I Award for his work on bistatic radar systems, algorithm development, and phenomenology and the 2012 IEEE Warren White Award for excellence in radar engineering. He is the Vice-Chair of the AES Radar Systems Panel and a fellow of AFRL (class of 2013).